chemistry

MDPI

Article

Multiple Intramolecular Hydrogen Bonding in Large Biomolecules: DFT Calculations and Deuterium Isotope Effects on ^{13}C Chemical Shifts as a Tool in Structural Studies

Poul Erik Hansen [1,*] and Fadhil S. Kamounah [2]

[1] Department of Science and Environment, Roskilde University, DK-4000 Roskilde, Denmark
[2] Department of Chemistry, University of Copenhagen, Universitetsparken 5, DK-2100 Copenhagen Ø, Denmark
* Correspondence: poulerik@ruc.dk

Abstract: Large biomolecules often have multiple intramolecular hydrogen bonds. In the cases where these interact, it requires special tools to disentangle the patterns. Such a tool could be deuterium isotope effects on chemical shifts. The use of theoretical calculations is an indispensable tool in such studies. The present paper illustrates how DFT calculations of chemical shifts and deuterium isotope effects on chemical shifts in combination with measurements of these effects can establish the complex intramolecular hydrogen bond patterns of rifampicin as an example) The structures were calculated using DFT theoretical calculations, performed with the Gaussian 16 software. The geometries were optimized using the B3LYP functional and the Pople basis set 6-31G(d) and the solvent (DMSO) was taken into account in the PCM approach. Besides the 6-31G(d) basis set, the 6-31 G(d,p) and the 6-3111G(d,p) basis sets were also tested. The nuclear shieldings were calculated using the GIAO approach. Deuteriation was simulated by shortening the X-H bond lengths by 0.01 Å.

Keywords: density functional calculations; deuterium isotope effects on chemical shifts; large biomolecules; intramolecular hydrogen bonding

Citation: Hansen, P.E.; Kamounah, F.S. Multiple Intramolecular Hydrogen Bonding in Large Biomolecules: DFT Calculations and Deuterium Isotope Effects on ^{13}C Chemical Shifts as a Tool in Structural Studies. *Chemistry* **2023**, *5*, 1317–1328. https://doi.org/10.3390/chemistry5020089

Academic Editor: Alessandro Ponti

Received: 30 March 2023
Revised: 15 May 2023
Accepted: 17 May 2023
Published: 23 May 2023

1. Introduction

Intramolecular hydrogen bonding is a very important structural parameter in many biomolecules, e.g., peptides, proteins, RNA, DNA and smaller molecules with specific biological effects such as rifampicin. [1]. Furthermore, the correct structure is a prerequisite for binding studies of molecules with biological activity [2] such as rifampicin. Rifampicin has important biological actions and is mentioned as a possible remedy against tuberculosis in combination with other drugs [3]. The introduction of deuterium in OH and NH groups is straightforward and is a minimal perturbation but still one that creates easily observable changes, e.g., in ^{13}C chemical shifts. Therefore, deuterium isotope effects on chemical shifts have turned out to be a useful tool in establishing the presence and the characteristics of intramolecular hydrogen bonds [4]. Examples include the use of deuterium isotope effects on ^{13}C chemical shifts as well as on ^{15}N chemical shifts in proteins [5,6]. Such isotope effects also have advantages in studies of DNA [7,8]. Intramolecular hydrogen bonding may also lead to tautomerism. This can also be studied with deuterium isotope effects on chemical shifts [9]. The situation can be complex in the cases in which several donors and acceptors forming hydrogen bonds with each other. Such a situation is found in rifampicin [2,10]. The use of theoretical calculations to calculate structures and NMR parameters have reached a very high level [11]. DFT calculations of structures, chemical shifts and isotope effects on chemical shifts combined with experimental values is particularly useful in the present study to disentangle the hydrogen bonding pattern of such a complex system as rifampicin and to determine if tautomerism is at play. Rifampicin has shown the very interesting feature that it may take up a zwitterionic form in polar solvents (Figure 1) [8]. Density

functional theory (DFT) calculations [12] are a very useful tool to analyze the complex situations both with regard to hydrogen bonding [13] and tautomerism [7]. Both nuclear shieldings and isotope effects on nuclear shieldings can be calculated [1]. Numerous examples of multiple hydrogen bonding involving biologically relevant structures can be found. Examples of calculations of structures and hydrogen bond energies including compounds with pyrroles were performed by the Afonin group [14–16].

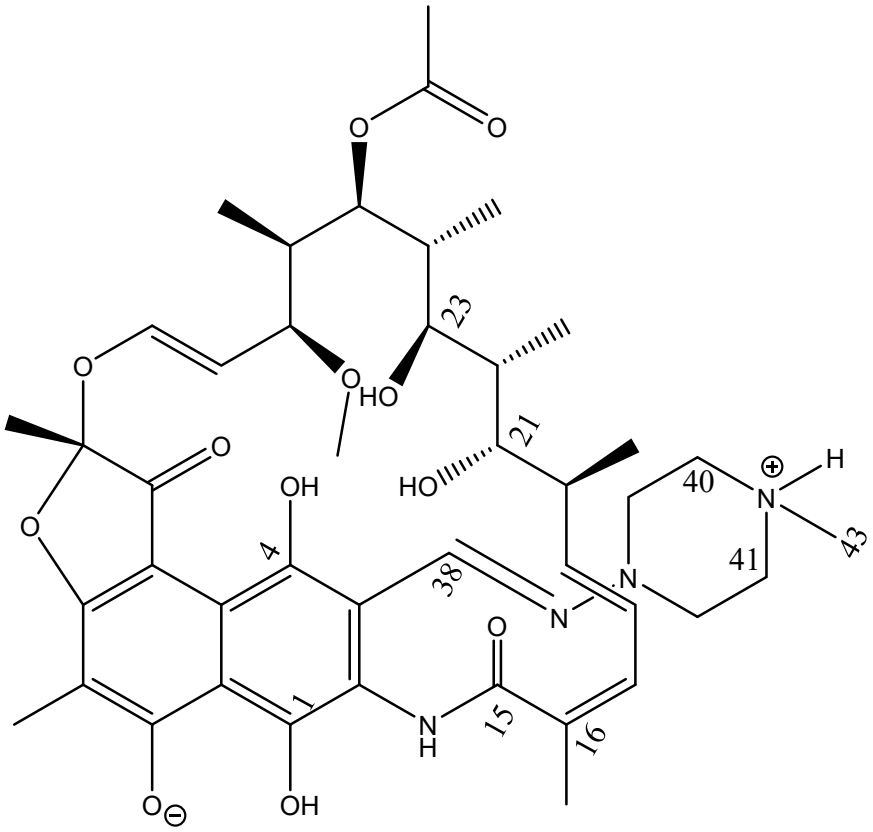

Figure 1. Rifampicin.

The measurement of deuterium isotope effects on chemical shifts can be performed in two different ways. If exchange of the label is slow, the measurement can be performed in a one-tube NMR experiment containing both isotopomers. However, if the exchange is fast, e.g., with presence of water, one can use a variation of the percentage of deuterium in the solvent, typically H_2O/D_2O or CH_3OH/CH_3OD, or use these as co-solvents in DMSO-d_6. Having performed experiments using 0 to 100% D_2O, the isotope effects can be obtained as the difference between these two situations. For systems showing changes upon the addition of water, the solvent effect of adding water must be determined. It is of course important to realize that the measured isotope effects are the sum of all possible unresolved isotope effects.

In the case of a tautomeric equilibrium, deuteriation will lead to a change in the chemical equilibrium. This, in turn, will lead to a change in the chemical shifts. This type of isotope effect mainly depends on the chemical shift differences of the same nucleus in the two equilibrating species and is hence a very good monitor of the existence of a tautomeric equilibrium.

The use of a combination of DFT calculations, and measurements of chemical shifts and isotope effects on ^{13}C chemical shifts is a general method that can be used in other biological systems, e.g., more complex derivatives of rifampicin such as the aldehyde [2].

2. Experimental

2.1. Calculations

The structures are calculated using DFT theoretical calculations [9] performed with the Gaussian 16 software [17]. The geometries were optimized using the B3LYP functional [18,19] and the Pople basis set 6-31G(d) [20], and the solvent (DMSO) was taken into account in the PCM [21,22] approach. X, Y, Z coordinates of structure A (see Section 3.4) are given in the Supplementary Materials. Besides the 6-31G(d) basis set, the 6-31 G(d,p) and the 6-3111G(d,p) basis sets were also tested. The nuclear shieldings were calculated using the GIAO approach [23,24]. Deuteration was simulated by shortening the X-H bond lengths by 0.01 Å [3].

2.2. NMR

One-dimensional ^{1}H and ^{13} C NMR spectra were recorded using a 300 MHz spectrometer (Bruker, Fallaenden, Germany) recorded at 300.08 MHz and 75.46 MHz, respectively in DMSO-d_6 using TMS as a reference. Examples of the ^{1}H and ^{13}C NMR spectra are shown in Sections 3.1 and 3.2.

2.3. Deuteration

Deuteration was achieved in a series of experiments by adding 2, 4 or 9 µL, and in some cases 20 or 30 µL, D_2O to the DMSO-d_6 solutions. The latter additions were used just to confirm that the effects at such high additions were linear. The solvent effects were estimated by the addition of 10 µL H_2O (see Section 3.4).

3. Results

3.1. ^{1}H NMR Spectrum

Both the OH-1 (15.6 ppm) and the NH+ (9.5 ppm) resonances were broad, indicating that they were in exchange. Those of OH-4 (12.5 ppm) and the NH amide (8.4 ppm) protons were sharp suggesting that these were not in exchange. An example of a ^{1}H NMR spectrum of a partially deuteriated species is shown in Figure 2. The degree of deuteriation was determined from the integrals of the exchangeable protons.

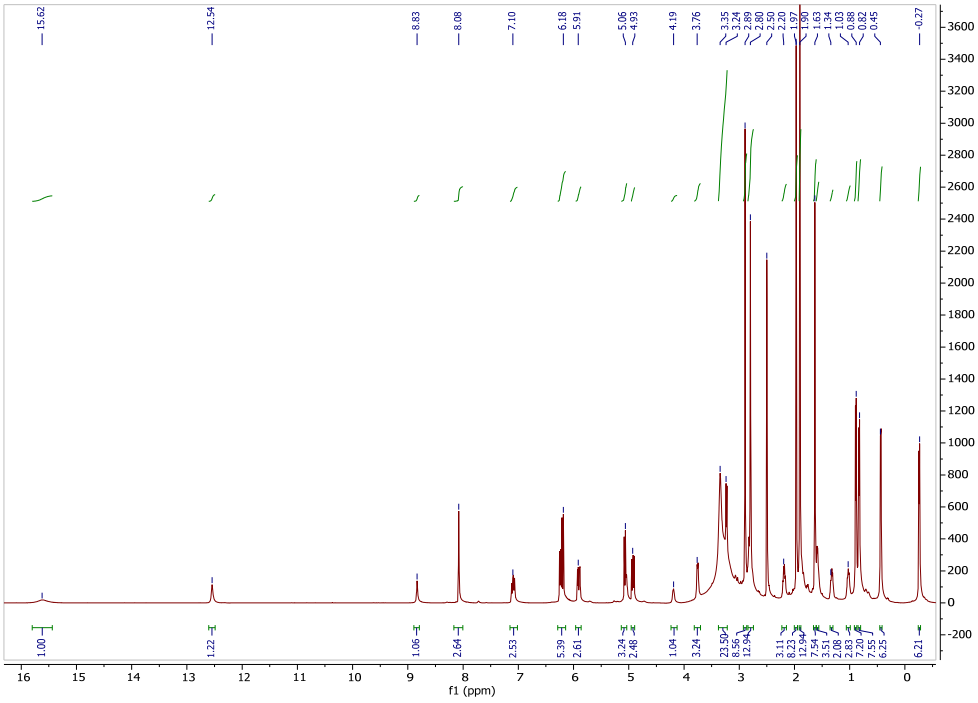

Figure 2. ^{1}H NMR spectrum of 45 mg rifampicin in 0.6 mL DMSO-d_6 + 4 µL D_2O.

3.2. ^{13}C NMR Spectrum

The ^{13}C NMR spectrum of rifampicin in $CDCl_3$ is given in [9]. The assignments used in this paper are very similar except for C-2, C-9 and C-10. A number of the resonances showed splittings due to deuteriation (see Table 1). The signs of the deuterium isotope effects on ^{13}C chemical shifts can be determined by knowing the degree of deuteriation. Other resonances showed a shift as a function of addition of D_2O (Table 1) (see Figure 3).

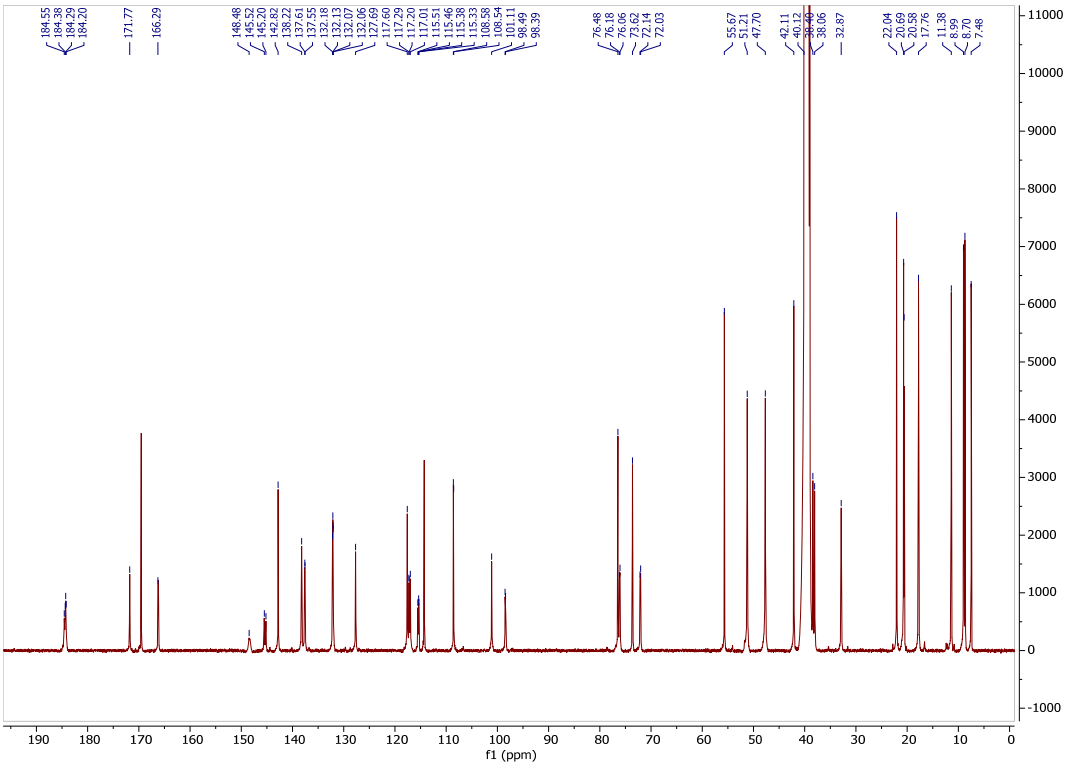

Figure 3. ^{13}C NMR spectrum of 45 mg rifampicin in 0.6 mL DMSO-d_6 + 4 µL D_2O.

Table 1. Observed and calculated deuterium isotope effects on ^{13}C chemical shifts in ppm measured in DMSO-d_6 as well as observed ^{13}C chemical shifts.

Carbon	^{13}C CS [a]	IE OH-1 [b]	IE H-4 [c]	IE NHCO [c]	IE NH^+ [d]	IE OH-21,23 [c]
C-1	148.52	0.33 (0.3)				
C-2 [d]	115.51		0.05 (0.07) [d]	0.13		
C-3	114.24					
C-4	145.40	−0.10 (−0.15)	0.31 (0.29)			
C-5	98.51	0.07 (0.08)	0.05 (0.09)			
C-6	171.77					
C-7	101.02		−0.09 (0.01)			
C-8	184.21		0.08 (0.09)			
C-9 [d]	117.21	−0.09 (−0.14)	0.0 (0.02)			
C-10 [d]	117.05	0.07 (−0.11)	0.07 (0.07)			
C-11	184.43	0.11 (0.07)	−0.17 (−0.10)			
C-12	108.55			0.042		
C-13						

Table 1. *Cont.*

Carbon	^{13}C CS [a]	IE OH-1 [b]	IE H-4 [c]	IE NHCO [c]	IE NH^{+} [d]	IE OH-21,23 [c]
C-14						
C-15	166.22			0.099		
C-16	132.17			0.046		
C-21						0.12
C-23						0.12
C-38	137.59	0.07 (0.03)				
C-40,41	51.21				0.07	
C-43	42.11				0.04 [e]	

[a] CS means chemical shift. [b] IE means isotope effect. These effects were determined as a change in the chemical shift upon D_2O addition (see Section 2). Only large effects are given. Values in brackets are calculated values. [c] Observed as splitting due to slow exchange of the label. Values in brackets are calculated values. [d] C-2, C-9 and C-10 are interchanged compared to [10]. [e] Slightly larger than 0.04 ppm.

3.3. Assignment of Isotope Effects on ^{13}C Chemical Shifts

In a system with several protons, which can be deuteriated, in this case OH-1, OH-4, NH+, OH-21, OH-23 and the NH amide proton, it is important to be able to determine which deuterium is causing which effect. In the ^{1}H spectrum, OH-1 and NH+ were broad, showing that they were easily exchanged and did not giving rise to observable deuterium isotope effects as doublets. This leaves the observable doublets as being due to OH-4, NHC=O, OH-21 and OH-23. The carbons of the latter two were in the aliphatic region and can be assigned. OH-21 and OH-23 were in a different part of the molecule and will not give rise to isotope effects on carbons of the aromatic rings. In an aliphatic system, the isotope effects are only transmitted over few bonds are thus very local. The effects due to NHC=O were local and restricted to C-2, C=O(NH) and C=C-16.

3.4. Isotope Effects

In a system like the present one, deuterium isotope effects on ^{13}C chemical shifts can be of different kinds. If the deuterium is slowly exchanged or not exchanged at all, intrinsic isotope effects are observed as splittings of the ^{13}C resonances. However, if the deuterium label is exchanged quickly, one observes only a change in the chemical shifts (see Table 2). Both these effects are intrinsic. Intrinsic isotope effects in aliphatic systems are only transmitted over a few bonds, whereas they can be transmitted over many bonds in conjugated systems like aromatic systems. [3] Intrinsic isotope effects are defined as:

$$^{n}\Delta C(D) = \delta C(H) - \delta C(D) \quad (1)$$

where n is the number of bonds between the label and the carbon in question.

However, if the system is tautomeric between two species, A and B, equilibrium isotope effects are observed. These are defined as:

$$^{n}\Delta X(D)_{int} = (1 - x)\ ^{n}\Delta X(D)_{A} + x\ ^{n}\Delta X(D)_{B} \quad (2)$$

$$^{n}\Delta X(D)_{eq} = (\delta X_{B} - \delta X_{A})\ \Delta x \quad (3)$$

$$^{n}\Delta X(D)_{OBS} = {}^{n}\Delta X(D)_{int} + {}^{n}\Delta X(D)_{eq} \quad (4)$$

In this case, X is ^{13}C and x is the mole fraction of B. Δx is the change in the equilibrium upon deuteration. The interesting part is that the equilibrium isotope effect depends on the chemical shift difference between the two sites ($\delta X_B - \delta X_A$).

Table 2. ^{13}C chemical shifts as a function of the addition of D_2O (H_2O) in μL.

	0 μL	**2 μL**	**4 μL**	**9 μL**	**20 μL**	**30 μL**	**10 μL** [a]
C11	184.43	184.37(H) [b] 184.57(D)	184.29(H) 184.51(D)	184.31(H) 184.47(D)	184.35(H) 184.55(D)	184.40(H) 184.60(D)	184.44(5)
C8	184.21	184.21(H) 184.13(D)	184.29 (H) 184.20 (D)	184.31 (D) 184.23(H)	184.30(D)	184.35(D)	184.25
C6	171.77	171.77	171.78	171.77	171.83	171.89	171.80
C35	169.48	169.49	169.51	169.54	169.64	169.72	169.53
C15	166.22	166.25	125.26	166.29	166.42	166.52	166.28
C1	148.52	148.45	148.34	148.28	148.28	148.32	148.57
C4	145.40	145.48(H) 145.17(D)	145.50(H) 145.19(D)	145.54(D) 145.21(H)	145.63(D) 145.32(H)	145.67(D) 145.36(H)	145.40
C29	142.79	142.79	142.81	142.82	142.89	142.94	142.80
C19	138.13	138.16	138.18	138.19	138.30	138.37	138.17
C38	137.59	137.60	137.54	137.49	137.54	137.55	137.55
C16	132.17	132.15	132.13	132.17	132.18	132.20	132.18
C17	131.99	132.02	132.05	132.06	-	-	132.03
C18	127.72	127.70	127.71	127.68	127.73	127.76	127.70
C28	117.59	117.58	117.58	117.56	117.63	117.67	117.61
C9	117.21	117.26(D) 117.17(H)	117.28(D) 117.20(H)	117.30(D) 117.21(H)	117.30(D) w [c] (H)	117.35 w(H)	117.23
C10	117.05	117.00	117.01	116.98	117.04	117.09	117.08
C2 [e]	115.51	115.48(HH) 115.44(DH) 115.34(HD) 115.31(DD)	115.48(HH) 115.44(DH) 115.36(DH) 115.31(DD)	115.46(HH) 115.42(DH) 115.33(HD) 115.29(DD)	115.35(DD)	115.51 [d] 115.38(DD)	115.51
C3	114.24	114.24	114.27	114.27	114.34	114.38	114.25
C12	108.55	108.55	108.57	108.57	108.62	108.67	108.57
C7	101.02	101.07	101.08	101.11	101.23	101.31	101.06
C5	98.51	98.48	98.46	98.44	98.42	98.48	98.54
C37	55.63	55.64	55.65	55.65	55.72	55.77	55.65
C40	51.21	51.17	51.19	51.18	51.24	51.27	51.25
C39	47.68	47.66	47.69	47.68	47.72	47.76	47.71
N-CH_3	42.11	42.07	42.09	42.09	42.14	42.21	42.16

[a] 10 μL water added to estimate the solvent effect of adding water/heavy water. [b] Refers to the resonance due to the H species and to the D deuterated species. [c] w means weak. [d] Only one weak signal observed. [e] Two deuterium isotope effects were observed.

The isotope effects on ^{13}C chemical shifts that are observed as doublets or doublets of doublets can be ascribed to deuteriation either at H-4, the NH or at OH-21 or OH-23 (see assignments, Section 3.3). As described earlier, the effects of deuteriation at the NH are restricted to C-2, C=O(NH) and C=C-16. The remaining observed isotope effects seen in Table 1 were due to deuteriation of OH-4. A plot of the experimental values vs. the calculated ones (see Section 3.5.2) showed a very good agreement (the structure is A of Figure 4). In contrast, a plot based on values of the structure C gave a correlation coefficient (R^2) as low as 0.38. In that case, see also the discussion on tautomerism.

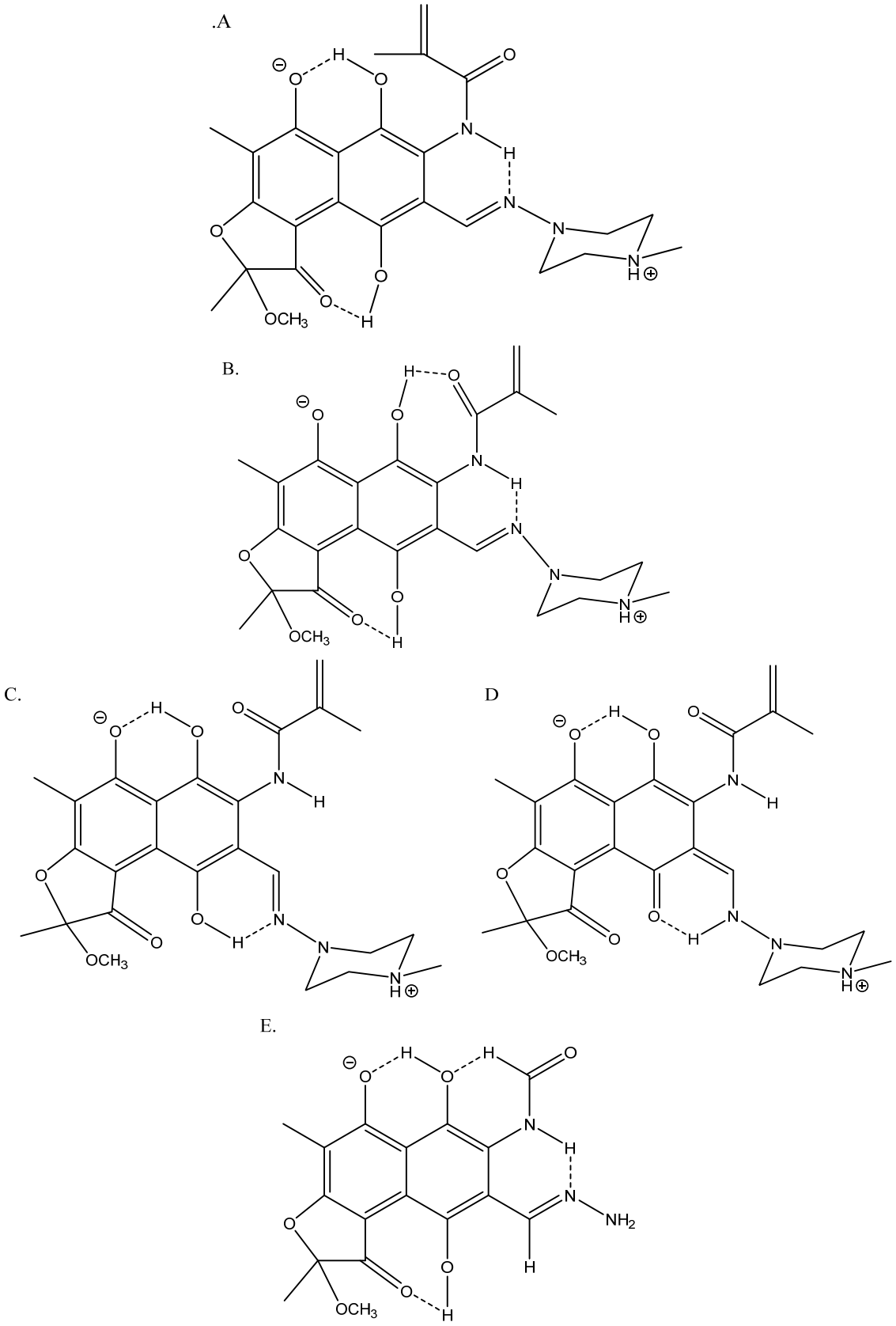

Figure 4. Truncated structures with different hydrogen bond motifs. More structures can clearly be constructed, but these are the most likely ones. Motifs: (**A**) OH-O^{-}, NH–N, OH-C=O; (**B**) OH-C=O, NH-N, OH-C=O; (**C**) OH-O^{-}, N-OH; (**D**) OH-O^{-}, NH-C=O; (**E**) Like A but with 1,4-piperazine ring replaced by NH_2 group.

Deuteriation at OH-1 did not lead to observable doublets. However, as described in Section 2.2, the isotope effects can be observed by measuring the shift as a function of D_2O addition. An example is shown for C-1 in Figure 5. From this plot, it can be seen that the addition of water in itself gave rise to a shift to a higher frequency. This has to be taken into account when estimating the isotope effect. The data are given in Table 2. Clearly, the largest observed isotope effects due to deuteriation occurred at OH-1. The other effects are given in Table 1. The smaller effects were somewhat more uncertain but the signs could, in all the mentioned cases, be determined. The observation of isotope effects for C-40, 41 and 43 was a clear confirmation that the structure was a zwitterion.

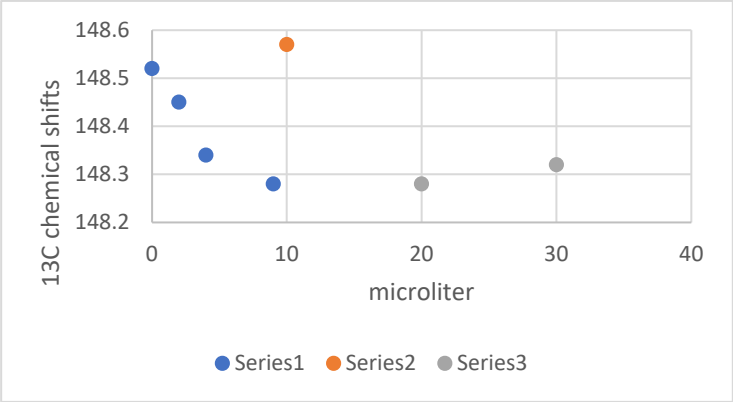

Figure 5. Plot of ^{13}C chemical shifts of C-1 vs. addition of heavy water (Series 1 and 3). Series 2 is the addition of H_2O.

In Table 2 it is important to notice that the C-2 doublet of doublets were observed due to isotope effects due to deuteriation both at OH-4 and NH.

3.5. Calculations

The structures were calculated using a truncated version of the molecule leaving out most of the long bridge. In one end, the double bond was kept and in the other end, the chain was replaced by a OCH_3 group (see Figure 4). Several structures were tested to obtain the optimal truncation. The test involved the fitting of calculated nuclear shieldings vs. observed ^{13}C chemical shifts (see Section 3.5.1). To determine the best basis set, 6-31G(d,p) and 6-311(G,p) were also tested. For structure 4A, the R^2 values were 0.9963 and 0.9935, respectively. If need be, the piperazine ring can be replaced by a NH_2 (Figure 4E) producing an R^2 of 0.9962. The structures were calculated with and without water molecules close to the O^- atom. The solvent was also taken into account (see Section 2).

3.5.1. ^{13}C Nuclear Shieldings

The calculated ^{13}C nuclear shieldings for structures C and D of Figure 4 are given in Table 3. The very large differences were related to C-4 and C-38.

A plot of the calculated ^{13}C nuclear shieldings vs. experimental ^{13}C chemical for structure A of Figure 4 is given in Figure 6 (R^2 = 0.9949). The carbons included are the core carbons C1-C10 and C-11. As carbons one and two bonds away heavily influence the chemical shifts, only the core carbons were involved as we were using the truncated version of the molecule. For the structure with a water molecule added to the O^-, R^2 = 0.9819. In other words, water did not seem to be bonded in the C1-C8 region. For structure C, R^2 = 0.9675, and for structure D, R^2 = 0.7884.

Table 3. ^{13}C nuclear shieldings for structures C and D of Figure 4.

Carbon	NS [a] of Structure C	NS of Structure D	Difference [b]
C-1	86.46	79.79	6.67
C-2	18.06	18.62	−0.56
C-3	73.73	77.66	−3.93
C-4	73.35	64.57	−21.22
C-5	94.86	90.29	4.57
C-6	24.91	26.62	−1.71
C-7	47.25	41.61	5.64
C-8	42.11	12.06	30.05
C-9	91.15	74.96	16.19
C-10	83.39	92.13	−8.74
C-14	11.64	10.14	1.50
C-19	36.79	37.93	−1.14
C-21	27.40	54.74	−27.34

[a] NS means nuclear shielding. [b] The differences were used to judge the possibility of finding an equilibrium isotope effect (see Section 4).

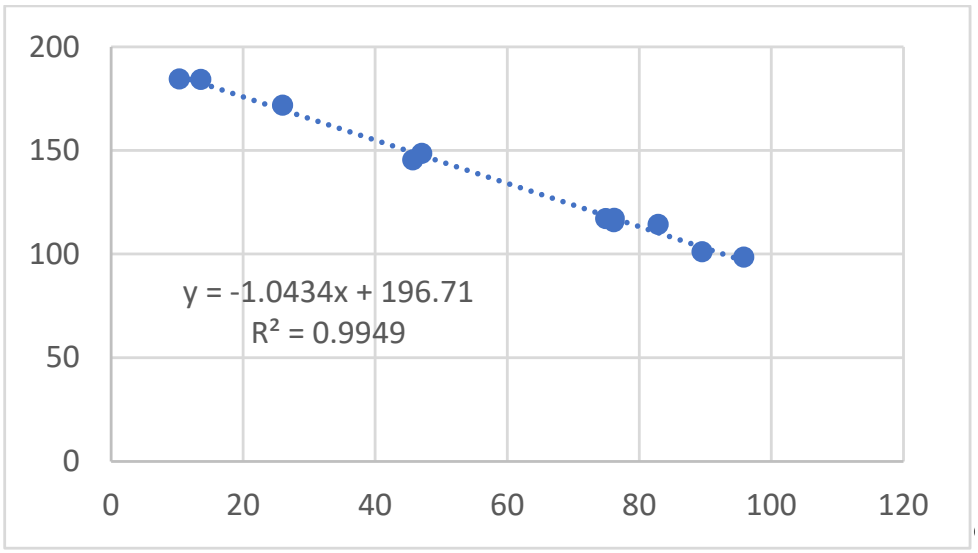

Figure 6. Plot of calculated vs. observed ^{13}C chemical shifts for structure A of Figure 4.

3.5.2. Isotope Effects on Chemical Shifts

The calculation of deuterium isotope effects on nuclear shieldings is based on the Jameson theory [25,26]. In the present case, the OH bond lengths were reduced by 0.01 Å to mimic the deuteriation [1]. This will lead to "standard" isotope effects that may need to be scaled by plotting those vs. the observed isotope effects. As seen in Table 1 and Figure 7, no scaling was needed for deuteriation of OH-4. A plot of the corresponding situation with water attached to O^- gave a slightly lower R^2 of 0.9723.

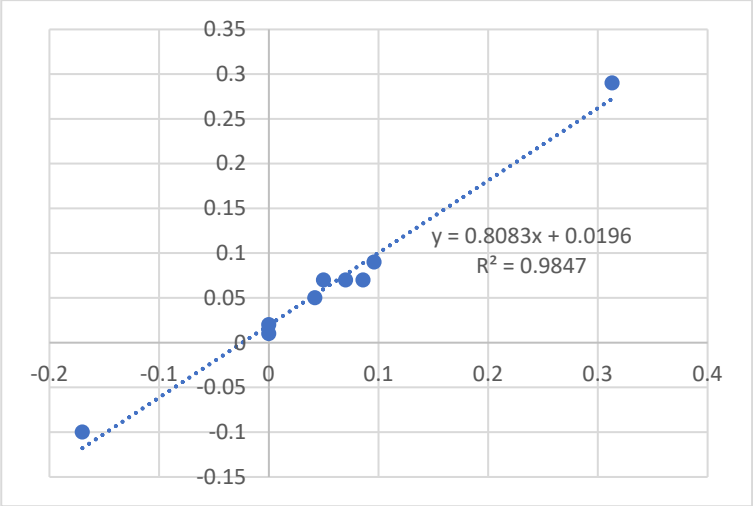

Figure 7. Plot of calculated deuterium isotope effects vs. observed isotope effects for deuteriation at OH-4. The data are based on structure 4A and with DMSO as the solvent.

4. Discussion

A breakthrough in understanding the structure of rifampicin (Figure 1) was the finding that the structure is a zwitterion in polar solvents with water added [8]. Taking this into account, a number of intramolecularly hydrogen bonded structures can be formulated as seen in Figure 4 (the structures are truncated versions of rifampicin).

These structures clearly demonstrate that changes in the intramolecular hydrogen bonding in one region will influence the hydrogen bonding pattern in another region. More structures with fewer hydrogen bonds can be drawn, but these are clearly less realistic.

Rifampicin is a large molecule. Here, the calculations were based on a truncated version including all essential features as seen in Figure 4. As water plays an important role in the formation of the zwitterionic form [7,8,27], water was added to the structure hydrogen bonding to C-O$^-$. This turned out to have very little effect on the calculated deuterium isotope effects of C-1 or C-4 or the ^{13}C nuclear shieldings (see Section 3.5.1). However, as water is important for the formation of the zwitterionic structure, the effect of water is to solvate the N$^+$ ammonium ion. This is very important as the counter ion is far away.

From the very high chemical shift of OH-1 (15.6 ppm), it can be concluded that OH-1 was hydrogen bonded to O$^-$. It was also seen that the OH-1 resonance was broad due to exchange.

With respect to OH-4, this can hydrogen bond to C=O in a seven-membered ring arrangement (Figure 4A or Figure 4E) or to the C=N in a six-membered arrangement (Figure 4C). However, in the latter case, it was very similar to *o*-hydroxy Schiff bases and can in principle be tautomeric [27] (see Figure 4D). However, in this case, one would expect distinctive equilibrium isotope effects at C-3, C-4, C-10 and C-38 proportional to the chemical shift differences between the carbons in the two equilibrating structures (see Equations (3) and (4)) [28]. The differences in calculated nuclear shielding are given in Table 3. Large isotope effects at C-3, C-4, C-10 and C-38 were clearly not seen in Table 1. Based on the finding that structure C was not fitting, that no equilibrium was established and the fact that the deuterium isotope effects on the ^{13}C chemical shifts of Figure 4A fits nicely (See Figure 5) makes 4A the likely structure. As OH-4 is hydrogen bonded to C-11=O, then the NH logically forms an intramolecular hydrogen bond to the nitrogen of the C=N bond. The observed $^2\Delta$C-2(ND) isotope effect of 0.133 ppm clearly showed that the NH was hydrogen bonded. Values of $^2\Delta$C-2(ND) for non-hydrogen bonded cases are typically 0.08–0.1 ppm [29,30]. Based on these arguments, a full structure similar to structures A or E of Figure 4 is the preferred one. Furthermore, this was confirmed by a comparison of experimental ^{13}C chemical shifts vs. calculated ^{13}C nuclear shieldings, as seen from the

R^2 of 0.9949, as discussed in Section 3.5.1. The isotope effects at C-40, 41 and 43 (Table 1) confirmed that rifampicin was in a zwitterionic form. These finding are similar to the full structure found in the crystal [9].

5. Conclusions

The search for a suitable basis set to use with the B3LYP functional resulted in G(d) giving good NMR nuclear shieldings and being suitable for the study of large biological systems. The DFT calculations were performed using the mentioned functional and basis set. The calculated nuclear shielding and deuterium isotope effects on ^{13}C nuclear shieldings combined with experimental ^{1}H and ^{13}C chemical shifts and deuterium isotope effects on the latter enabled an analysis of the complex hydrogen bonding pattern of the zwitterionic form of rifampicin. The result was an extended hydrogen bonding network determined to a large extent on the hydrogen bond between O^- and OH-1. The deuterium isotope effects on nuclear shieldings also confirmed the zwitterionic nature of rifampicin in polar solvents.

Supplementary Materials: The following supporting information can be downloaded at: https://www.mdpi.com/article/10.3390/chemistry5020089/s1, Figure S1: Expanded ^{13}C NMR spectra. Table S1: x, y, z coordinates.

Author Contributions: Conceptualization, P.E.H.; methodology, P.E.H.; writing—original draft preparation, P.E.H.; writing—review and editing, F.S.K. All authors have read and agreed to the published version of the manuscript.

Funding: This research received no external funding.

Data Availability Statement: Not applicable.

Acknowledgments: The authors would like to thank Annette Christensen for the expert recording of the NMR spectra and P. Przybylski for his help.

Conflicts of Interest: The authors declare no conflict of interest.

References

1. Pyta, K.; Janas, A.; Skrzypczak, N.; Schilf, W.; Wicher, B.; Gdaniec, M.; Bartl, F.; Przybylski, P. Specific Interactions between Rifamycin Antibiotics and Water Influencing Ability to Overcome Natural Cell Barriers and the Range of Antibacterial Potency. *ACS Infect. Dis.* **2019**, *5*, 1754–1763. [CrossRef] [PubMed]
2. Kozyra, P.; Kaczor, A.; Karczmarzyk, Z.; Wysocki, W.; Pitucha, M. Experimental and computational studies of tautomerism pyridine carbonyl thiosemicarbazide derivatives. *Struct. Chem.* **2023**. [CrossRef]
3. Pyta, K.; Przybylski, P.; Klich, K.; Stefańska, J. A new model of binding of rifampicin and its amino analogues as zwitterionsto bacterial RNA polymerase. *Org. Biomol. Chem.* **2012**, *10*, 8283–8297. [CrossRef] [PubMed]
4. Hansen, P.E. Isotope Effects on Chemical shifts of small molecules. *Molecules* **2022**, *27*, 2405. [CrossRef]
5. Hansen, P.E. Isotope Effects on Chemical Shifts of Proteins and Peptides. *Magn. Reson. Chem.* **2000**, *38*, 1–10. [CrossRef]
6. Hansen, P.E. Isotope Effects on Chemical Shifts in the Study of Hydrogen Bonded Biological Systems. *Progress NMR* **2020**, *120–121*, 109–117. [CrossRef]
7. Kim, Y.-I.; Manalo, M.N.; Perés, M.L.; LiWang, A. Computational and empirical trans-hydrogen bond deuterium isotope shifts suggest that N1–N3 A: U hydrogen bonds of RNA are shorter than those of A:T hydrogen bonds of DNA. *J. Biomol. NMR* **2006**, *34*, 229–236. [CrossRef]
8. Manalo, M.N.; Perés, L.M.; LiWang, A. Hydrogen-bonding and base-stacking interactions are coupled in DNA, as suggested by Calculated and experimental trans-Hbond deuterium isotope effects. *J. Am. Chem. Soc.* **2007**, *129*, 11298–11299. [CrossRef]
9. Hansen, P.E. Methods to distinguish tautomeric cases from static ones. In *Tautomerism: Ideas, Compounds, Applications*; Antonov, L., Ed.; Wiley-VCH: Weinheim, Germany, 2016.
10. Pyta, K.; Przybylski, P.; Wicker, B.; Gdaniec, M.; Stefańska, J. Intramolecular proton transfer impact on antibacterial properties of ansamycin antibiotic rifampicin and its new amino analogues. *Org. Biomol. Chem.* **2012**, *10*, 2385–2388. [CrossRef]
11. Morgante, P.; Peverat, R. The devil in the details: A tutorial review on some undervalued aspects of density functional theory calculations. *Quantum Chem.* **2020**, *120*, e26332. [CrossRef]
12. Becke, A.D. Density-Functional Thermochemistry. III. The Role of Exact Exchange. *J. Chem. Phys.* **1993**, *98*, 5648–5652. [CrossRef]
13. Ireta, J.; Neugebauer, J.; Scheffler, M. On the Accuracy of DFT for Describing Hydrogen Bonds: Dependence on the Bond Directionality. *J. Phys. Chem. A* **2004**, *108*, 5692–5698. [CrossRef]

14. Afonin, A.V.; Ushakov, I.A.; Simonenko, D.E.; Shmidt, E.Y.; Zorina, N.V.; Mikhaleva, A.I.; Trofimov, B.A. ^{1}H and ^{13}C NMR Study of Bifurcated Intramolecular Hydrogen Bonds in 2,6-Bis(2-pyrrolyl)pyridine and 2,6-Bis(1-vinyl-2-pyrrolyl)pyridine. *Russ. J. Org. Chem.* **2005**, *41*, 1516–1521, Translated from Zhurnal Organicheskoi Khimii, Vol. 41, No. 10, 2005. [CrossRef]
15. Afonin, A.V.; Vashchenko, A.V.; Ushakov, I.A.; Zorina, N.V.; Schmidt, E.Y. Comparative analysis of hydrogen bondingwith participation of the nitrogen, oxygen andsulfur atoms in the 2(2-heteroaryl)pyrroles andtheir trifluoroacetyl derivatives based on the ^{1}H,^{13}C,^{15}N spectroscopy and DFT calculations. *Magn. Reson. Chem.* **2008**, *46*, 441–447. [CrossRef]
16. Afonin, A.V.; Vashchenko, A.V.; Sigalov, M.V. Estimating the energy of intramolecular hydrogenbonds from ^{1}H NMR and QTAIM calculations. *Org. Biomol. Chem.* **2016**, *14*, 11199. [CrossRef] [PubMed]
17. Frisch, M.J.; Trucks, G.W.; Schlegel, H.B.; Scuseria, G.E.; Robb, M.A.; Cheeseman, J.R.; Scalmani, G.; Barone, V.; Petersson, G.A.; Nakatsuji, H.; et al. *Gaussian 16, Revision C.01*; Gaussian, Inc.: Wallingford, CT, USA, 2016.
18. Becke, A.D. Density-functional exchange-energy approximation with correct asymptotic behavior. *Phys. Rev. A* **1988**, *38*, 3098–3100. [CrossRef] [PubMed]
19. Lee, C.; Yang, W.; Parr, R.G. Development of the Colle-Salvetti correlation-energy formula into a functional of the electron density. *Phys. Rev. B* **1988**, *37*, 785–789. [CrossRef]
20. Ditchfield, R.; Hehre, W.J.; Pople, J.A. Self-consistent Molecular-orbital methods. 9. Extended Gaussian-type Basis for Molecular-Orbital Studies of Organic Molecules. *J. Chem. Phys.* **1971**, *54*, 724–728. [CrossRef]
21. Miertus, S.; Scrocco, E.; Tomasi, J. Electrostatic interaction of a solute with a continuum. A direct utilization of AB initio molecular potentials for the prevision of solvent effects. *Chem. Phys.* **1981**, *55*, 117–129. [CrossRef]
22. Scalmani, G.; Frisch, M.J. Continuous surface charge polarizable continuum models of solvation. I. General formalism. *J. Chem. Phys.* **2010**, *132*, 114110. [CrossRef]
23. Ditchfield, R. Self-consistent perturbation theory of diamagnetism. I. A gauge-invariant LCAO method for N.M.R. chemical shifts. *Mol. Phys.* **1974**, *27*, 789–807. [CrossRef]
24. Wolinski, K.; Hilton, F.F.; Pulay, P. Efficient implementation of the gauge-independent atomic orbital method for NMR chemical shift calculations. *J. Am. Chem. Soc.* **1990**, *112*, 8251–8260. [CrossRef]
25. Jameson, C.J.; Osten, H.-J. The NMR isotope shift in polyatomic molecules. Estimation of the dynamic factors. *J. Chem. Phys.* **1984**, *81*, 4300–4305. [CrossRef]
26. Jameson, C.J. *Isotopes in the Physical and Biomedical Sciences. Isotopic Applications in NMR Studies*; Buncel, E., Jones, J.R., Eds.; Elsevier: Amsterdam, The Netherlands, 1991.
27. Dziembowska, T.; Rozwadowski, Z.; Filarowski, A.; Hansen, P.E. A multinuclear NMR study of proton transfer equilibrium in Schiff bases derived from 2-hydroxy-1-naphtaldehyde. Deuterium isotope effects on ^{13}C and ^{15}N chemical shifts. *Magn. Reson. Chem.* **2001**, *39*, S67–S80. [CrossRef]
28. Filarowski, A.; Koll, A.; Rospenk, M.; Krol-Starzomska, I.; Hansen, P.E. Tautomerism of sterically hindered Schiff bases. Deuterium Isotope Effects on ^{13}C Chemical Shifts. *J. Phys. Chem. A* **2005**, *109*, 4464–4473. [CrossRef] [PubMed]
29. Jarret, M.; Sin, N.; Dintzner, M. Deuterium Isotope Effects on^{13}C NMR Chemical Shifts of Amides. *Microchem. J.* **1997**, *56*, 19–21. [CrossRef]
30. Newmark, R.A.; Hill, J.R. Assignment of Primary and Secondary Amide Carbonyl Resonances in Carbon-13 NMR. *J. Magn. Reson.* **1976**, *21*, 1–7. [CrossRef]